analytical chemistry

ARTICLE

pubs.acs.org/ac

Hydrogen Peroxide Sensing with Horseradish Peroxidase-Modified Polymer Single Conical Nanochannels

Mubarak Ali,[*,†,⊥] Muhammad Nawaz Tahir,[‡] Zuzanna Siwy,[§] Reinhard Neumann,[⊥] Wolfgang Tremel,[‡] and Wolfgang Ensinger[†]

[†]Technische Universität Darmstadt, Fachbereich Material-u. Geowissenschaften, Fachgebiet Materialanalytik, Petersenstrasse 23, D-64287 Darmstadt, Germany

[‡]Department of Chemistry, Johannes Gutenberg-Universität, Duesbergweg 10-14, 55099 Mainz, Germany

[§]Department of Physics and Astronomy, University of California, Irvine, California 92697, United States

[⊥]GSI Helmholtzzentrum für Schwerionenforschung, Planckstrasse 1, D-64291 Darmstadt, Germany

ABSTRACT: Inspired from the funtioning and responsiveness of biological ion channels, researchers attempt to develop biosensing systems based on polymer and solid-state nanochannels. The applicability of these nanochannels for detection/sensing of any foreign analyte in the surrounding environment depends critically on the surface characteristics of the inner walls. Attaching recognition sites to the channel walls leads to the preparation of sensors targeted at a specific molecule. There are many nanochannel platforms for the detection of DNA and proteins, but only a few are capable of detecting small molecules. Here, we describe a nanochannel platform for the detection of hydrogen peroxide, H_2O_2, which is not only a toxic waste product in the cellular systems but also a key player in the redox signaling pathways. The sensor is based on single conical nanochannels fabricated in an ion tracked polymer membrane. The inner walls of the channel are decorated with horseradish peroxidase (HRP) enzyme using carbodiimide coupling chemistry. The success of the HRP immobilization on the channel surface is confirmed by measuring the pH-dependent current−voltage ($I-V$) curves of the system. The reported HRP-nanochannel system detects nanomolar concentrations of H_2O_2 with 2,2′-azino-bis(3-ethylbenzothiazoline-6-sulfonate) (ABTS) as the substrate. The immobilized HRP enzyme is thus capable of inducing redox reactions in a subfemtoliter volume of single nanochannels. We demonstrate that functioning of the designed biosensor is reversible and can be used multiple times to detect H_2O_2 at various concentrations.

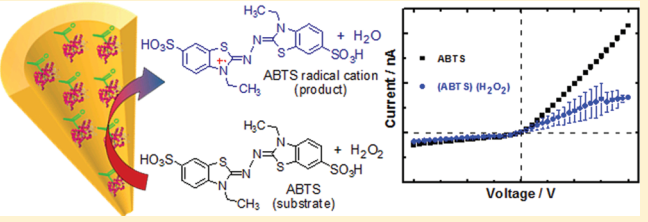

Nature has inspired scientists and engineers to miniaturize electrochemical devices having applications in various sensing and separation processes, including manipulation of single molecules.[1−12] Ion channels in a cell membrane regulate the flow of ions and molecules across the cell boundaries.[13] Many biological channels are selective for a given ion or molecule and are responsive so that the transport is regulated by changes in the electrical potential difference/pressure or by the binding of a chemical to the channel structure. Biological channels have also become a model system to investigate transport phenomena at the nanoscale.[14,15] The first sensor for DNA and proteins was based on the bacterial channel α-hemolysin.[5,16−18]

Synthetic nanochannels have recently attracted a great deal of interest because their geometry and surface chemistry can be fully controlled. They also feature excellent mechanical robustness and compatibility with various electronic measurement systems. Synthetic nanochannels fabricated in polymer and silicon-based films as well as glass nanopipettes have already been applied for the detection of DNA and protein analytes.[3,19−22] Solid-state nanochannels functionalized with suitable recognition elements (e.g., antibody or DNA strands) have been demonstrated as a sensor targeted at a given molecule (e.g., antigen).[5,10,23−29] Translocating molecules bind with the recognition chemical groups on the channel walls, which are detected as a change of transport properties of the system.

Here, we would like to present another type of nanoporous hydrogen peroxide (H_2O_2) sensor based on single conical polymer nanochannels whose walls are functionalized with the horseradish peroxidase (HRP) enzyme. The immobilized enzyme remains active in redox reactions that occur inside a single nanochannel in the presence of even nanomolar concentrations of H_2O_2. Monitoring the redox reactions via changes of the nanochannel transport properties offers an easy method to detect H_2O_2. Hydrogen peroxide has been recognized as an agent whose quantitative monitoring would be important for medical diagnostics. It is because accumulation of H_2O_2 in the mitochondria, for example, can lead to cancer as well as neurodegenerative diseases such as Alzheimer's, Parkinson's, and Huntington's

Received: October 24, 2010
Accepted: January 8, 2011
Published: February 04, 2011

diseases.[30−33] On the contrary, H_2O_2 has also been identified as a messenger in various signaling pathways.[34]

A variety of quantitative methods have already been developed for the detection of H_2O_2. The most commonly used approaches include chemical and biological techniques, based on spectrometry,[35−38] chemoluminescence,[39−44] amperometry,[45−49] and electrochemistry.[50−55] The conventional spectrometric and chemoluminescence methods are generally time-consuming; they require expensive reagents (e.g., fluorescent tags) and equipment. Many of the electrochemical techniques to detect H_2O_2 rely on the direct oxidation of the molecule using metal, e.g., Pt electrodes. These systems do not always offer optimal conditions for the H_2O_2 detection due to their poor selectivity, low sensitivity and electrode fouling.[56−59] In addition, oxidation of H_2O_2 requires overpotentials at which other electroactive species might interfere with the detection. Another electrochemical method to detect H_2O_2 involves redox-active mediators, but in some cases, the observed electrochemical response cannot be easily correlated with the H_2O_2 concentration. Lyon and Stevenson used an indicator molecule (Amplex Red) that becomes electrochemically active only when chemically oxidized by H_2O_2 in the presence of HRP enzyme.[59] HRP catalyzed the decomposition of H_2O_2 to peroxy radicals which subsequently were reduced to water via chemical oxidation of Amplex Red to resorufin. Resofurin was then electrochemically detected at the electrode. The system, although offering an excellent detection limit of ∼10 pM, was susceptible to electrode fouling and required cleaning the electrode between measurements. The electrochemical biosensors typically involve an electrode material onto which HRP[49,59,60] or cytochrome c[61] enzymes are immobilized. Direct contact between the enzyme and the electrode was, however, found to cause potential structural and functional changes of the enzymes, which also influenced the detection.[62,63] Leaching of the enzymes from the electrode is another important issue which seriously imparts a sensor function. To mitigate these problems, Peng et al.[52] used a mixed monolayer of ferrocenylalkanethiol and encapsulated horseradish peroxidase (HRP) at a gold electrode which prevented the enzyme leaching and avoided a direct contact of the enzyme with the electrode.

Confining the sensing reaction into a volume of a single-nanochannel offers a simple method to detect H_2O_2 and solves many of the challenges of the previous H_2O_2 sensors. The advantages of the nanoporous sensors include easiness of the HRP attachment and excellent detection limit and sensitivity, as well as the possibility to follow a function of a single or a few enzyme molecules. The sensor would not be susceptible to fouling because the products of the redox reaction could be designed to be removed by the applied electric field. In the proposed system, the detection signal would also be very easy to follow by simply using a picoammeter and voltage source. Here, we demonstrate a system in which H_2O_2 is detected via a redox reaction induced by the H_2O_2 molecules in a single conical nanochannel fabricated in ion tracked polymer membranes. The HRP enzyme was covalently attached to the inner walls of the nanochannels by amide linkage to the inherent carboxyl (−COOH) groups generated on the surface of as-fabricated nanochannels. The successful enzyme immobilization was confirmed by measuring the pH-dependent current−voltage ($I-V$) characteristics before and after the HRP attachment. $I-V$ curves of conical nanochannels strongly depend on the surface charge of the channel walls, which became modified upon HRP attachment. Addition of H_2O_2 to the electrolyte solution led to further changes of the transmembrane current induced by the formation of charged products of the redox reaction.

The following redox system with HRP and H_2O_2 was realized inside a single conical channel. In the presence of H_2O_2, the HRP enzyme immobilized on the channel walls is rapidly converted into an oxidized peroxidase form known as compound I (oxidation state: +5), containing oxy-ferryl heme (Fe^{4+}=O) and a porphyrin cation radical (reaction 1 below). The porphyrin cation radical in compound I accepts one electron from the reducing substrate molecule to generate compound II (oxidation state: +4) which retains the heme in the ferryl (Fe^{4+}=O) state (reaction 2). Subsequently, compound II is reduced back to the resting enzyme via one electron transfer from another substrate molecule (reaction 3).[64,65] This catalytic reaction induces the oxidation of the substrate to its corresponding radical cation species. As a substrate, we used 2,2′-azino-bis(3-ethylbenzothiazoline-6-sulfonate) (ABTS) substrate, expecting the formation of $ABTS^{\bullet+}$ product.

$$\mathrm{HRP(Fe^{3+})Porp} + \mathrm{H_2O_2} \rightarrow \underset{\text{Compound I}}{\mathrm{HRP(Fe^{4+}{=}O)Porp^{\bullet+}}} + \mathrm{H_2O} \quad (1)$$

$$\mathrm{HRP(Fe^{4+}{=}O)Porp^{\bullet+}} + \mathrm{AH} \rightarrow \underset{\text{Compound II}}{\mathrm{HRP(Fe^{4+}{=}O)Porp}} + \mathrm{A^{\bullet}} \quad (2)$$

$$\mathrm{HRP(Fe^{4+}{=}O)Porp} + \mathrm{AH} \rightarrow \mathrm{HRP(Fe^{3+})Porp} + \mathrm{A^{\bullet}} + \mathrm{H_2O} \quad (3)$$

The cationic products of the redox reactions accumulated in a single nanochannel and caused changes in the transmembrane ionic transport monitored by measuring the $I-V$ curves and signals of ion current in time. Due to the subfemtoliter volume of single nanochannels, small nM amounts of H_2O_2 could already be detected.[66−68] This contribution also indicates the possibility of studying functionality of enzyme molecules inside a single nanochannel.

RESULTS AND DISCUSSION

Single conical nanochannels were fabricated in 12 μm thick films of polyethylene terephthalate (PET) by the track-etching technique. The technique is based on first irradiating polymer films with single swift heavy ions, followed by the selective chemical etching of the damage trails caused by the ions along their trajectories. The conical shape of the channels resulted from the asymmetric development of the damaged tracks in a concentrated sodium hydroxide (NaOH) solution.[69,70] The chemical etching process as well as electrochemical characterization of fabricated nanochannels were performed in a two-chamber conductivity cell. As a result of the heavy ion irradiation and chemical etching, carboxyl (−COOH) groups are generated on the membrane surface and the channel walls with a density of ∼1 group per nm^2.[71] These inherent −COOH groups can be used as a starting point for introduction of other functionalities to the channel walls using the amide linkage between −COOH groups and amines. Here, we present linkage of the −COOH groups with primary amines of the HRP enzyme. The reaction was performed from a water solution of *N*-(3-dimethylaminopropyl)-*N*′-ethylcarbodiimide

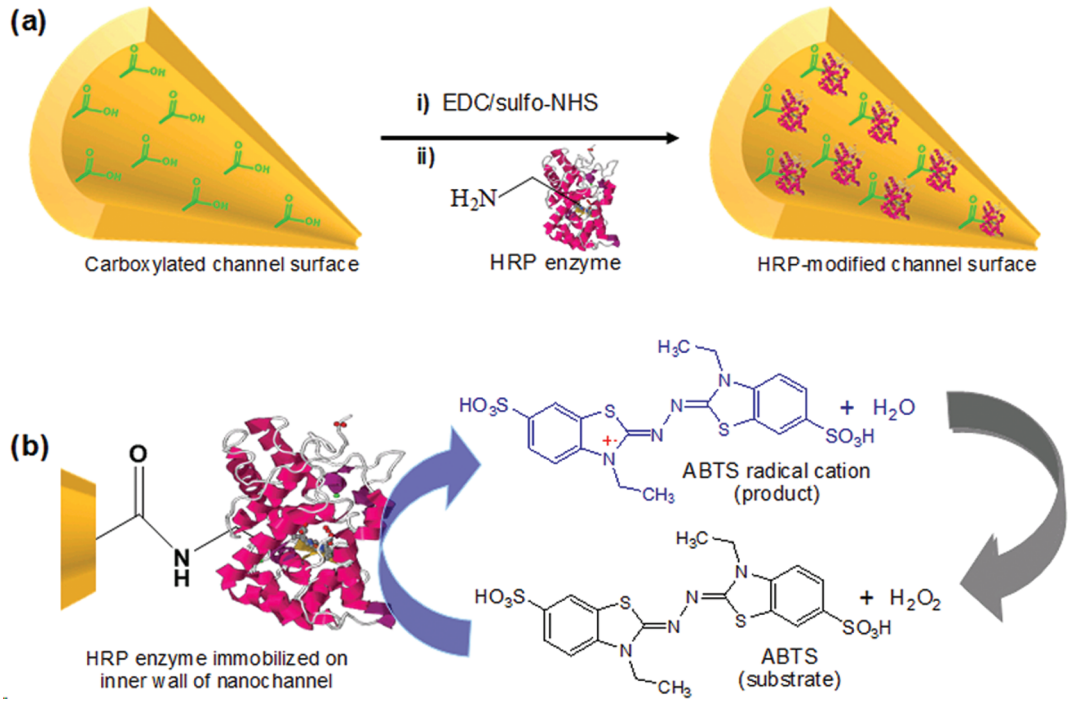

Figure 1. Performing redox reactions in a single conical nanochannel. (a) Schematic representation of a covalent attachment of the horseradish peroxidase (HRP) enzyme to carboxyl groups in a single conical nanochannel via carbodiimide coupling chemistry. (b) Scheme of the biocatalyzed redox reaction of the immobilized HRP enzyme leading to the conversion of ABTS into respective radical cation product in the presence of hydrogen peroxide. The crystal structures of horseradish peroxidase (HRP) enzyme was obtained from Protein Data Bank (ID: 1H5M.pdb).[94]

HCl (EDC) and *N*-hydroxysulfosuccinimide (sulfo-NHS).[72] The EDC reagent first activated the −COOH groups into a highly reactive *o*-acylisourea intermediate. This intermediate was further converted into a more stable sulfo-succinimidyl amine-reactive ester in the presence of excess sulfo-NHS ester molecules. Subsequently, the succinimidyl intermediate was covalently coupled with the ε-NH_2 of lysine residues in HRP molecules to form stable amide bonds (Figure 1).

The success of the functionalization procedure was confirmed by measuring the current−voltage ($I-V$) characteristics of a single conical nanochannel prior to and after the enzyme immobilization (Figure 2). The recordings were performed in symmetric electrolyte conditions on both sides of the membrane using 0.1 M KCl solution as an electrolyte, buffered to different pH values as indicated in Figure 2. It is well-known that conically shaped nanochannels at pH > 4.0 are cation selective and rectify the cation current with the preferential direction of the ion flow from the narrow opening to the wide opening of a cone.[73−75] In our electrode configuration, higher currents are recorded for positive voltages. For negative voltages, the cations flow from the wide opening toward the narrow tip of the cone, and the negative currents are lower. Rectification properties of the nanochannels can be quantified by calculating the rectification degree (f_{rec}) defined as the ratio of absolute values of ion currents measured at voltages of the same amplitude but opposite polarities. Rectification degree at pH 6.5 for the nanochannel presented in Figure 2a is ∼13 at 2 V. It is important to mention that ion current rectification properties are only pronounced at conditions at which the nanochannel behavior is influenced by the presence of the electrical double layer.[73−75] Well-defined ion current rectification behavior, presented in Figure 2a, confirms nanoscale opening of the channel.[76−80]

Ion current rectification is strongly dependent on the surface charge of the channel walls, which can be regulated by the solution pH.[69] Lowering pH from 6.5 to 4.5 diminished the positive current of the nanochannel at +2 V from 3.9 to 2.6 nA (Figure 2), while the negative currents remained unchanged. Eventually, at pH = 3.0, the same channel behaved like an ohmic resistor indicating that the net surface charge on the channel walls was zero (Figure 2a).[81−83] Change of the ion current rectification with pH were explained before via pH-dependent ionic concentrations in the channel.[76−80]

As expected, immobilization of the HRP enzyme caused partial blockage of the channel observed as lowering of the transmembrane ionic current (Figure 2b). It is known that HRP has a molecular weight of approximately 44 kDa and is ∼3.6 nm in diameter;[84] thus, its attachment into our ∼20 nm in diameter channel was expected to diminish the effective channel opening. Ion current for +2 V dropped from 3.9 nA before to ∼1 nA after the HRP attachment. Similarly, ion current measured at the reverse bias, i.e., −2 V, also decreased from 300 to ∼100 pA (Figure 2b). The decrease in the recorded current could also occur due to the change in the surface charge density induced by the HRP attachment, which we studied at different pH values.

The rectification degree at pH 6.5 and 2 V of the HRP-nanochannel system (f_{rec} = 11) is similar to the value of f_{rec} calculated prior to the HRP attachment (f_{rec} = 13). This observation suggests that, at pH 6.5, the HRP molecules did not significantly alter the average surface charge density of the system.

Due to the amphoteric character of the HRP enzyme, the HRP-nanochannel system exhibited a strong dependence of its transport properties on the solution pH. At pH = 6.5, the

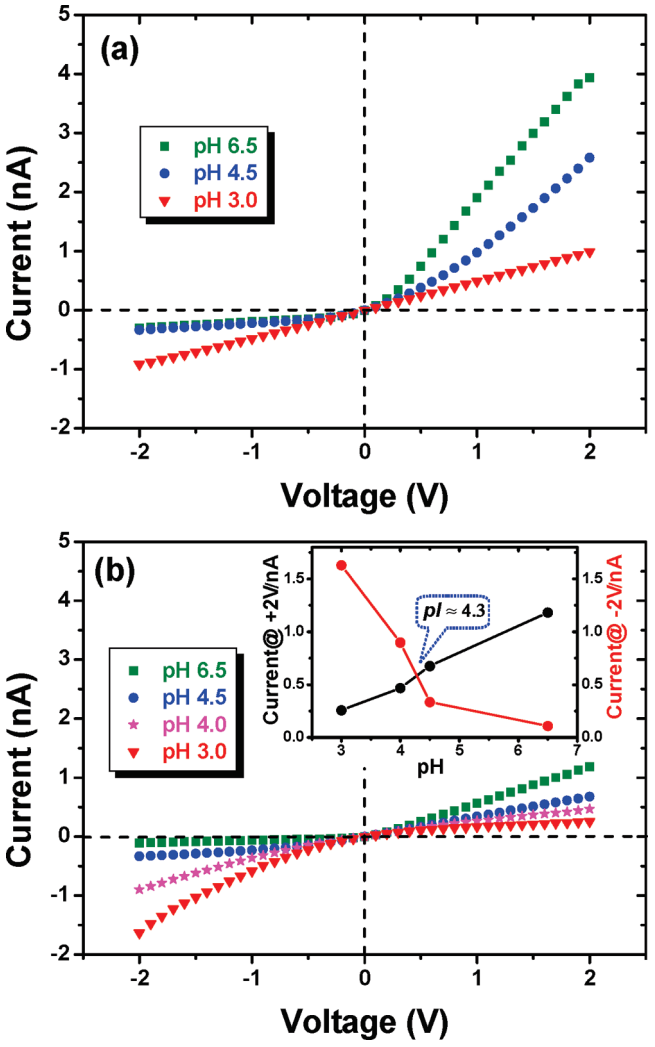

Figure 2. Current−voltage ($I-V$) characteristics of a single conical nanochannel in 0.1 M KCl buffered to different pH values as indicated in the (a) before and (b) after functionalization of the channel walls with HRP enzyme. The diameter of the channel tip before HRP immobilization was ∼19 nm. The inset in (b) summarizes the changes of ion currents with solution pH at +2 V (black symbols) and −2 V (red symbols) for the HRP-modified system. The pH value at which positive and negative currents have the same magnitude indicates pI of the HRP enzyme.

HRP-decorated channel still showed an asymmetric $I-V$ curve with positive currents higher than the negative currents. However, in an acidic solution (pH = 3.0), the current−voltage curve is flipped so that the values of negative currents became higher than those of positive currents (Figure 2b). This qualitative change in the $I-V$ curve for the modified channel indicated the switching of the surface charge from negative at pH 6.5 to positive at pH 3.0. The surface charge switch is indeed expected in the case of a successful HRP attachment, since at acidic pH the enzyme becomes positively charged due to the protonation of the terminal ε $-NH_2$ of lysine residues and N-termini in the enzyme molecules. In acidic conditions, the inner walls of the HRP-modified channel are thus positively charged, resulting in the anionic selectivity of the channel as well as in the inversion of rectification characteristics. The rectification degree at pH 3 calculated as $I(-2\text{ V})/I(+2\text{ V})$ was 6.3. Therefore, the shape of $I-V$ curves acts as an indicator for the surface charge polarity.[77,80]

At pH values between 6.5 and 4.5, the HRP-modified channel showed rectification with positive current values higher than negative currents, indicating the net negative surface charge of the channel walls. Rectification degree at pH 4.5, calculated as $I(+2\text{ V})/I(-2\text{ V})$, was equal to 6.3. At pH 4.0, however, the $I-V$ curve reversed and the rectification degree determined as $I(-2\text{ V})/I(+2\text{ V})$ was only 1.8. This significant loss in rectification displayed by the channel indicated that pH 4 was close to the isoelectric point (pI ∼ 4.3) of the amphoteric immobilized HRP isozyme (inset to Figure 2b). It is well-known that HRP enzymes have at least seven isozymes whose isoelectric points can be very different in the range between 3.0 and 9.0.[85,86] Studying $I-V$ curves of HRP-modified channels at a wide range of pH values provides the possibility to determine the pI value of the particular isozyme used in the experiments by finding a solution at which the nanochannel does not rectify the current.[28,77,81]

The pH-dependent behavior of the rectifying $I-V$ curves, measured for the HRP-nanochannel system, provided evidence for the successful enzyme immobilization on the nanochannel walls. As the next step, we investigated that the immobilized enzyme was active in redox reactions performed in the confined volume of a single nanochannel. The immobilized HRP enzyme was tested in a system containing 2,2′-azino-bis(3-ethylbenzothiazoline-6-sulfonate) (ABTS) as a substrate along with hydrogen peroxide (H_2O_2) as an analyte. Figure 3 shows the transmembrane current through a single HRP-modified channel, recorded in the presence of the substrate ABTS (1.5 mM) dissolved in 0.1 M KCl (pH = 6.5) prior to and after the addition of H_2O_2. In the absence of H_2O_2, $I-V$ curves were smooth and very similar to those recorded in just KCl solution (Figure 2b). Addition of 0.5 mM H_2O_2 induced a significant decrease of positive currents, which also became more unstable. For positive voltages, the measured $I-V$ curves additionally exhibited a hysteresis: the currents for voltages increasing from 0 V to +2 V were significantly higher than the recordings for the voltage sweep from +2 to 0 V (Figure 3a). We attributed the current changes to the appearance of cationic products of the redox reaction that occurred in the presence of HRP, ABTS, and H_2O_2.[87,88] The measurements also indicated that the reaction products obstructed the ion current flow through the channel, as it is discussed later.

When designing a sensing platform, it is very important to demonstrate its reversibility as well as sensitivity to low concentrations of an analyte. Therefore, we repeated the measurements of $I-V$ curves using the same electrolyte (0.1 M KCl + 1.5 mM ABTS) solution in the presence or absence of H_2O_2 analyte. The recordings were performed by manually changing the solutions in the conductivity cell used for the ion current measurements. Figure 3b presents the reversible variation of the transmembrane ionic current measured at +2 V without and in the presence of H_2O_2. The measurements confirmed excellent reversibility of the sensor: the same nanochannel could indeed be used for multiple sensing experiments without any loss of the sensing signal and with very good reproducibility (Figure 3b).

Figure 4 presents current−voltage curves of the HRP-nanochannel system in the presence of ABTS and various concentrations of H_2O_2 in the background electrolyte solution. The current scales with the H_2O_2 concentration in a linear fashion; thus, the presented platform also gives quantitative information on the H_2O_2 concentration down to nanomolar (Figure 4). The

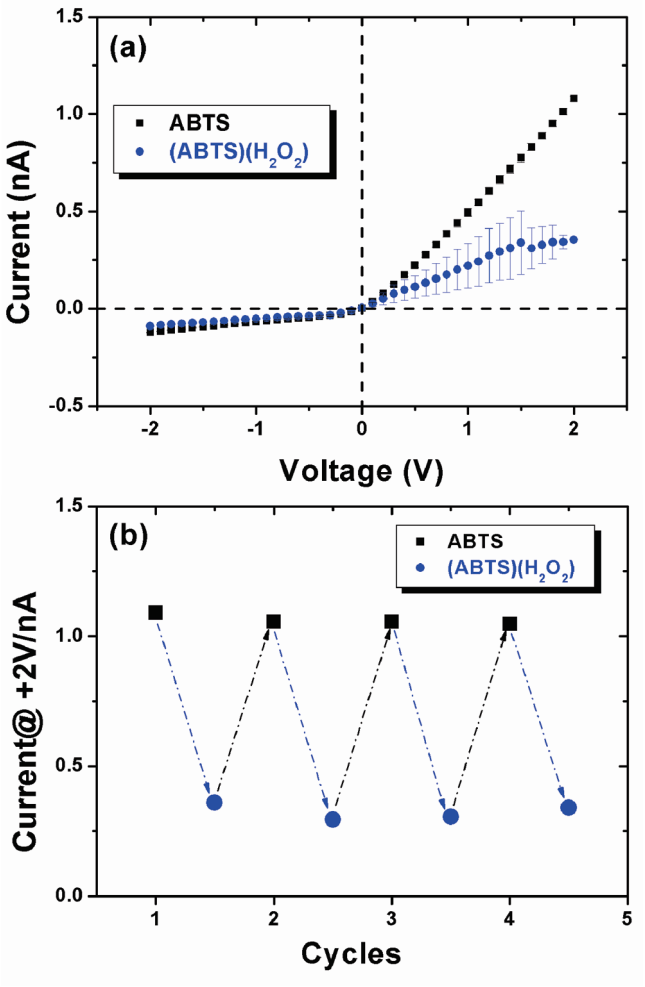

Figure 3. Response of the HRP-nanochannel system to H_2O_2. (a) Current−voltage ($I-V$) characteristics of a single HRP-modified channel recorded in the absence (■) and in the presence (blue ●) of 0.5 mM hydrogen peroxide in 0.1 M KCl solution containing 1.5 mM ABTS substrate. (b) Reversible variation of the transmembrane ionic current measured at +2 V with 0.1 M KCl containing 1.5 mM ABTS with (blue ●) and without (■) 0.5 mM hydrogen peroxide. The solutions were exchanged manually. The diameter of the narrow opening of this channel before HRP attachment was 19 nm.

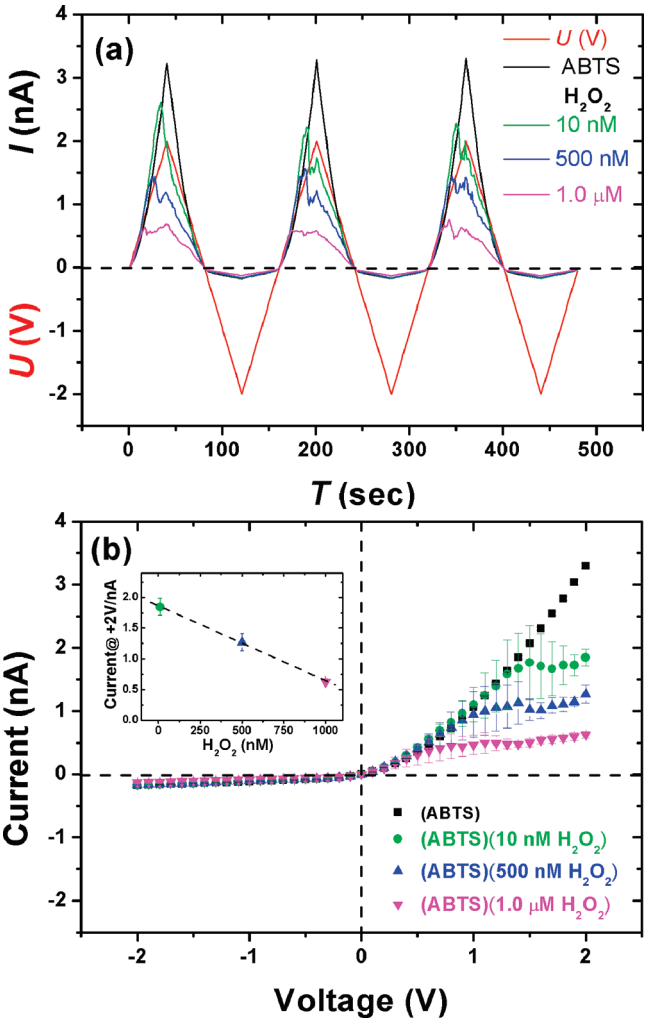

Figure 4. (a) Applied voltage and measured current signals in time together with (b) the corresponding current−voltage ($I-V$) characteristics of a single asymmetric nanochannel functionalized with the HRP enzyme. The recordings were performed in an electrolyte solution containing 1.5 mM ABTS and various concentrations of hydrogen peroxide: 0 nM (black), 10 nM (green), 500 nM (blue), and 1.0 μM (pink), respectively. The tip diameter of the nanochannel before HRP functionalization was 26 nm. The inset summarizes the changes of ion currents versus H_2O_2 concentration at +2 V.

slope of the linear dependence is ~1.5 ± 0.2 pA per 1 nM of H_2O_2. Our experimental setup to measure ion current can easily recognize a 10 pA change in the current flowing across the membrane. The presented platform is therefore expected to measure H_2O_2 concentration with ~10 nM precision.

However, the question still remains: what makes the HRP-nanochannel system respond to different H_2O_2 concentrations? We think that the ion current decrease together with the current instabilities observed with the HRP-modified channel are caused by the products of the redox reactions occurring in the nanochannel in the presence of H_2O_2 and ABTS as the substrate. Addition of H_2O_2 initiated oxidation and reduction reactions between HRP and ABTS analyte molecules,[88] resulting in the generation of the cationic radicals ($ABTS^{\bullet+}$) product. We would like to mention two possible scenarios of how the redox reaction products can affect the transmembrane current. (1) At pH 6.5, the cationic radicals ($ABTS^{\bullet+}$) electrostatically interact with the negative surface charges of the walls, causing fluctuations of the surface charge density. It was reported that transient changes of the charge of channel walls were responsible for ion current fluctuations in PET nanochannels.[89,90] Higher concentrations of H_2O_2 resulted in the generation of a larger amount of $ABTS^{\bullet+}$, which ultimately enhances the transient neutralization of the charges on the channel surface and consequently lowers the ionic currents.[69−71] (2) The cationic products of the redox reaction $ABTS^{\bullet+}$[87,91] might also cause steric obstruction of the nanochannel, which will be more pronounced at higher concentrations of H_2O_2. The radical cation ($ABTS^{\bullet+}$) molecules might compete with K^+ ions during their translocation through the narrow opening of the nanochannel so that there is an elevated concentration of $ABTS^{\bullet+}$ at the channel tip region. The $ABTS^{\bullet+}$ concentration is additionally enhanced by the applied voltage. It is known that, for conically shaped nanochannels with negative surface charges and external voltages that drive cations from the tip toward the wide opening of the cone, the cation concentration

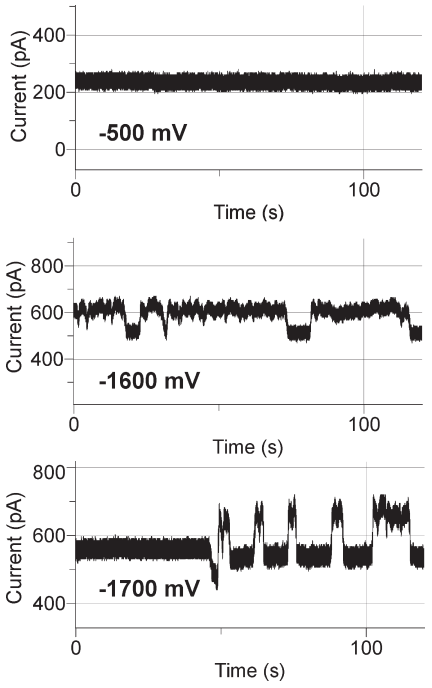

Figure 5. Examples of time series of ion current recorded through a single conical nanochannel modified with HRP enzyme. The recordings were performed in a solution of 0.1 M KCl at pH 6.5, containing 1.5 mM ABTS and 0.5 mM H_2O_2. Diameter of this conical nanochannel before the HRP attachment was 12 nm.

at the tip is at least several times higher than the bulk concentration.[74,92] For voltages of the opposite polarity, the tip region of the channel contains depleted cation concentration, which explains the lack of effect of the redox reactions for negative voltages.

It is also possible that electrostatic and steric effect of $ABTS^{\bullet+}$ molecules can act in concert to produce the observed ion current changes. Electrostatic adsorption of $ABTS^{\bullet+}$ to the channel walls would additionally enhance the radical concentration in the channel and at the same time cause a decrease of the effective surface charge density of the channel walls and channel obstruction.[93] Both effects will result in the decrease of the current. Driving the accumulated $ABTS^{\bullet+}$ out of the channel does not happen instantaneously as indicated by the current hysteresis on ramping the voltage down from +2 to 0 V.

The instabilities of ion current in the HRP-nanochannel system, in the presence of H_2O_2 (Figure 4a), prompted us to investigate the transient recordings of the ion current for a constant voltage. The stability of the current signal is important in building a reversible and reproducible sensor system. We also expected that, for sufficiently narrow nanochannels, one could potentially observe discrete current openings and closings due to the presence of a small number of the cation radical $ABTS^{\bullet+}$ blocking the channel. Figure 5 shows the transient ion current recordings through a single conically shaped nanochannel with HRP, in the presence of ABTS and H_2O_2. The observed fluctuations did not exceed 20% of the signal and were rather slow (Figure 5). We observed several occurrences of the current switching in a 2 min recording. The sensing signals induced by the addition of H_2O_2 showed much larger current changes than the current instabilities (e.g., 1 μM H_2O_2 induced ~5-fold decrease of ion current at +2 V for a channel with tip diameter ~26 nm used in present study (Figure 4b)). These measurements confirm the sufficient stability of the current signal and suggest that the observed current changes most probably constitute a collective effect of many $ABTS^{\bullet+}$ molecules being driven through the channel.

CONCLUSIONS

In conclusion, we have presented a single nanochannel system whose walls were decorated with covalently linked enzyme HRP. The function of the immobilized enzyme in a single nanochannel as an H_2O_2 sensor was confirmed by studying products of the redox reactions occurring in the presence of the substrates ABTS and various concentrations of H_2O_2. We found that the cationic radical $ABTS^{\bullet+}$ reduced the ion current in the HRP-nanochannel in a voltage-dependent fashion, consistent with voltage-dependent concentrations of ions in conical nanochannels. The magnitude of the current blockage was correlated with the H_2O_2 concentration in the solution. The current response scaled linearly over a wide range of the H_2O_2 concentrations from micromolar to nanomolar. The sensor sensitivity is predicted to reach the level of ~10 nM, which is superior over many existing H_2O_2 sensors[53,54] but lower than the best electrochemical sensing devices presented thus far (~10 pM).[52,59] Our nanoporous system, however, is simple to prepare, is not susceptible to fouling, and can be used multiple times without the loss of the sensing signal. The covalent HRP attachment prevents the enzyme leaching. We also expect that using narrower pores will allow lowering the detection limit and improve the sensor sensitivity. We also showed that studying current−voltage curves of the HRP-nanochannel at solutions of different pHs gives information on the isoelectric point of the enzyme.

The presented HRP-nanochannel allows studying the function of the enzyme in a subfemtoliter volume of a single nanochannel. The small volume induces accumulation of the redox reaction products in the channel, which helps to improve the detection limits. Using nanochannels of even smaller diameter might allow us to detect redox reaction products of only one HRP molecule. The detection signal relies on $I-V$ curves, which are much less susceptible to external noise than the time-resolved detection of molecules.[5] The detection can also be observed with off-the-shelf electronic equipment.

MATERIALS AND METHODS

Polymer Foils and Chemicals. Polymer films of polyethylene terephthalate (PET; Hostaphan RN 12, Hoechst) of 12 μm thickness were irradiated at the linear accelerator UNILAC (GSI, Darmstadt) with single swift heavy ions (Pb, U, and Au) having an energy of 11.4 MeV per nucleon.

Chemicals. *N*-(3-Dimethylaminopropyl)-*N*′-ethylcarbodiimide hydrochloride (EDC, 98%, Fluka), *N*-hydroxysulfosuccinimide (sulfo-NHS, 98.5+ %, Aldrich), peroxidase from horseradish (HRP, Sigma), 2,2′-azino-bis(3-ethylbenzthiazoline-6-sulfonic acid) (ABTS, 98.5+ %, Sigma), hydrogen peroxide (H_2O_2, 30%, SL Labor-Service), potassium chloride (KCl, 99.99%, Merck), and the surfactant Dowfax* 2A1 (Dow Chemical) were used as received.

Fabrication of Asymmetric Nanochannels. The fabrication of single nanochannels in 12 μm thick PET films was performed by the track-etching technique. After irradiating the films with energetic single ions, one side of the films was treated with soft

UV light for 35 h. We used a UV source that provides light intensities of ∼1.5 and 4 W m^{-2} in the wavelength ranges of 280−320 nm and 320−400 nm, respectively. Subsequently, the film was placed between two halves of a conductivity cell with the seal resistance exceeding 100 GΩ. The UV-sensitized side of the membrane was in contact with a pure etchant (6 M NaOH), while the other side of the membrane was in contact with a protecting solution containing 4 M NaOH and 0.02% v/v surfactant. The etching process was carried out at 60 °C under the applied voltage of −1 V.[69,70] The etching current remained zero as long as the channel was not etched through (∼30 s), and after the breakthrough, an increase of ionic current through the nascent channel was observed. The etching process was stopped when the current reached a value of ∼10 nA. The channel was washed first with 1 M HCl in order to quench the etchant, followed by rinsing with deionized water.

After etching, the diameter of the large opening (D) of the channel was determined by field emission scanning electron microscopy (FESEM). For this purpose, a PET sample containing 10^7 channels cm^{-2} was etched simultaneously with the single channel under the same conditions. The diameter of the small opening (d) was estimated by assuming a conical geometry of the channel using the following relation[69]

$$d = 4LI/\pi D\kappa V$$

where L is the length of the channel which could be approximated to the thickness of the membrane, d and D are the small and large opening diameters of the channel, respectively, κ is the specific conductivity of the electrolyte (1.313 S/m for 0.1 M KCl at 26 °C), V is the voltage applied across the membrane, and I is the measured current.

Functionalization with HRP Enzyme. The solutions used for the chemical modification of the channel surface were prepared in 0.1 M MES buffer [2-(*N*-morpholino) ethanesulfonic acid], pH = 5.5. Functionalization of nanochannel walls with HRP was carried out in the same conductivity cell that was used for etching of tracked polymer films. The carboxyl groups of the channel walls were first activated into sulfo-NHS-esters in a 10 mM solution of *N*-(3-dimethylaminopropyl)-*N*′-ethylcarbodiimide hydrochloride (EDC) and 20 mM *N*-hydroxysulfosuccinimide (sulfo-NHS) for 30 min. After the activation, the foil was washed with the MES buffer solution. As the next step, the amine-reactive sulfo-NHS-esters were covalently coupled with the primary amine groups present in the horseradish peroxidase molecule (HRP, 1 mg/mL) in a reaction carried out overnight. Finally, the modified channel was washed thoroughly with buffer solution.

Ion Current Measurements. Single nanochannel membranes were mounted between two halves of the conductivity cell and both halves of the cell were filled with 0.1 M KCl solution buffered to pH values between 6.5 and 3.0. An Ag/AgCl electrode was placed into each half-cell solution, and a picoammeter/voltage source (Keithley 6487, Keithley Instruments, Cleveland, OH) was used to apply the desired transmembrane potential and measure the current. The ground electrode was placed at the side of the membrane with the big opening of the channel. In order to record current−voltage curves, a scanning triangle voltage signal from −2 V to +2 V was used. Ion current signals in time were recorded using the amplifier Axopatch 200B connected to the computer via the analog-to-digital converter Digidata 1322A (Molecular Devices, Inc.).

AUTHOR INFORMATION

Corresponding Author
*E-mail: m.ali@gsi.de.

ACKNOWLEDGMENT

M.A., R.N., and W.E. gratefully acknowledge financial support by the Beilstein-Institut, Frankfurt/Main, Germany, within the research collaboration NanoBiC. Z.S. is grateful to the Alexander von Humboldt Foundation for the Friedrich Wilhelm Bessel Award and the National Science Foundation (CHE 0747237, CMMI 825661). M.N.T and W.T. are thankful to the Deutsche Forschungsgemeinschaft, the Bundesministerium für Bildung und Forschung, Germany [Center of Excellence BIOTECmarin], the European Society for Marine Biotechnology, and the International Human Frontier Science Program for their financial support.

REFERENCES

(1) Baker, L. A.; Bird, S. P. *Nat. Nanotechnol.* **2008**, *3*, 73–74.
(2) Duan, C.; Majumdar, A. *Nat. Nanotechnol.* **2010**, *5*, 848–852.
(3) Healy, K.; Schiedt, B.; Morrison, A. P. *Nanomedicine* **2007**, *2*, 875–897.
(4) Hou, X.; Jiang, L. *ACS Nano* **2009**, *3*, 3339–3342.
(5) Howorka, S.; Siwy, Z. *Chem. Soc. Rev.* **2009**, *38*, 2360–2384.
(6) Jirage, K. B.; Hulteen, J. C.; Martin, C. R. *Science* **1997**, *278*, 655–658.
(7) Mara, A.; Siwy, Z.; Trautmann, C.; Wan, J.; Kamme, F. *Nano Lett.* **2004**, *4*, 497–501.
(8) Martin, C. R.; Siwy, Z. S. *Science* **2007**, *317*, 331–332.
(9) Savariar, E. N.; Krishnamoorthy, K.; Thayumanavan, S. *Nat. Nanotechnol.* **2008**, *3*, 112–117.
(10) Siwy, Z.; Trofin, L.; Kohli, P.; Baker, L. A.; Trautmann, C.; Martin, C. R. *J. Am. Chem. Soc.* **2005**, *127*, 5000–5001.
(11) Ali, M.; Yameen, B.; Neumann, R.; Ensinger, W.; Knoll, W.; Azzaroni, O. *J. Am. Chem. Soc.* **2008**, *130*, 16351–16357.
(12) Ali, M.; Neumann, R.; Ensinger, W. *ACS Nano* **2010**, 7267–7274.
(13) Hille, B. *Ionic channels of excitable membranes*, 3rd ed.; Sinauer Associates Inc.: Sunderland, MA, 2001.
(14) Alcaraz, A.; Nestorovich, E. M.; Aguilella-Arzo, M.; Aguilella, V. M.; Bezrukov, S. M. *Biophys. J.* **2004**, *87*, 943–957.
(15) Alcaraz, A.; Ramirez, P.; Garcia-Gimenez, E.; Lopez, M. L.; Andrio, A.; Aguilella, V. M. *J. Phys. Chem. B* **2006**, *110*, 21205–21209.
(16) Han, A. P.; Schurmann, G.; Mondin, G.; Bitterli, R. A.; Hegelbach, N. G.; de Rooij, N. F.; Staufer, U. *Appl. Phys. Lett.* **2006**, *88*, 093901.
(17) Kasianowicz, J. J.; Brandin, E.; Branton, D.; Deamer, D. W. *Proc. Natl. Acad. Sci. U.S.A.* **1996**, *93*, 13770–13773.
(18) Movileanu, L. *Trends Biotechnol.* **2009**, *27*, 333–341.
(19) Dekker, C. *Nat. Nanotechnol.* **2007**, *2*, 209–215.
(20) Gyurcsanyi, R. E. *TrAC, Trends Anal. Chem.* **2008**, *27*, 627–639.
(21) Rhee, M.; Burns, M. A. *Trends Biotechnol.* **2007**, *25*, 174–181.
(22) Siwy, Z. S.; Howorka, S. *Chem. Soc. Rev.* **2010**, *39*, 1115–1132.
(23) Ali, M.; Schiedt, B.; Neumann, R.; Ensinger, W. *Macromol. Biosci.* **2010**, *10*, 28–32.
(24) Bayley, H.; Cremer, P. S. *Nature* **2001**, *413*, 226–230.
(25) Fologea, D.; Gershow, M.; Ledden, B.; McNabb, D. S.; Golovchenko, J. A.; Li, J. L. *Nano Lett.* **2005**, *5*, 1905–1909.
(26) Harrell, C. C.; Kohli, P.; Siwy, Z.; Martin, C. R. *J. Am. Chem. Soc.* **2004**, *126*, 15646–15647.
(27) Hou, X.; Guo, W.; Xia, F.; Nie, F. Q.; Dong, H.; Tian, Y.; Wen, L. P.; Wang, L.; Cao, L. X.; Yang, Y.; Xue, J. M.; Song, Y. L.; Wang, Y. G.; Liu, D. S.; Jiang, L. *J. Am. Chem. Soc.* **2009**, *131*, 7800–7805.
(28) Vlassiouk, I.; Kozel, T. R.; Siwy, Z. S. *J. Am. Chem. Soc.* **2009**, *131*, 8211–8220.

(29) Wanunu, M.; Meller, A. *Nano Lett.* **2007**, *7*, 1580–1585.
(30) Barnham, K. J.; Masters, C. L.; Bush, A. I. *Nat. Rev. Drug Discovery* **2004**, *3*, 205–214.
(31) Dickinson, B. C.; Chang, C. J. *J. Am. Chem. Soc.* **2008**, *130*, 9638–9639.
(32) Finkel, T.; Serrano, M.; Blasco, M. A. *Nature* **2007**, *448*, 767–774.
(33) Lin, M. T.; Beal, M. F. *Nature* **2006**, *443*, 787–795.
(34) Jin, H.; Heller, D. A.; Kalbacova, M.; Kim, J. H.; Zhang, J. Q.; Boghossian, A. A.; Maheshri, N.; Strano, M. S. *Nat. Nanotechnol.* **2010**, *5*, 302–309.
(35) Chang, Q.; Zhu, L. H.; Jiang, G. D.; Tang, H. Q. *Anal. Bioanal. Chem.* **2009**, *395*, 2377–2385.
(36) Dickinson, B. C.; Huynh, C.; Chang, C. J. *J. Am. Chem. Soc.* **2010**, *132*, 5906–5915.
(37) Jin, H.; Heller, D. A.; Kalbacova, M.; Kim, J. H.; Zhang, J. Q.; Boghossian, A. A.; Maheshri, N.; Strano, M. S. *Nat. Nanotechnol.* **2010**, *5*, 302–U381.
(38) Srikun, D.; Albers, A. E.; Nam, C. I.; Iavaron, A. T.; Chang, C. J. *J. Am. Chem. Soc.* **2010**, *132*, 4455–4465.
(39) Chen, W. W.; Li, B. X.; Xu, C. L.; Wang, L. *Biosensor. Bioelectron.* **2009**, *24*, 2534–2540.
(40) Diaz, A. N.; Peinado, M. C. R.; Minguez, M. C. T. *Anal. Chim. Acta* **1998**, *363*, 221–227.
(41) Qin, W.; Zhang, Z. J.; Li, B. X.; Liu, S. N. *Anal. Chim. Acta* **1998**, *372*, 357–363.
(42) Rubtsova, M. Y.; Kovba, G. V.; Egorov, A. M. *Biosens. Bioelectron.* **1998**, *13*, 75–85.
(43) Tahirovic, A.; Copra, A.; Omanovic-Miklicanin, E.; Kalcher, K. *Talanta* **2007**, *72*, 1378–1385.
(44) Zhang, Z. Y.; Zhang, S. C.; Zhang, X. R. *Anal. Chim. Acta* **2005**, *541*, 37–47.
(45) Bustos, E. B.; Chapman, T. W.; Rodriguez-Valadez, F.; Godinez, L. A. *Electroanalysis* **2006**, *18*, 2092–2098.
(46) Kausaite-Minkstimiene, A.; Mazeiko, V.; Ramanaviciene, A.; Ramanavicius, A. *Bioelectron. Bioelectron.* **2010**, *26*, 790−797.
(47) Nakabayashi, Y.; Yoshikawa, H. *Anal. Sci.* **2000**, *16*, 609–613.
(48) Quintino, M. S. M.; Winnischofer, H.; Araki, K.; Toma, H. E.; Angnes, L. *Analyst* **2005**, *130*, 221–226.
(49) Zhang, Y. Y.; Yuan, R.; Chai, Y. Q.; Xiang, Y.; Hong, C. L.; Ran, X. Q. *Biochem. Eng. J.* **2010**, *51*, 102–109.
(50) Lee, D. Y.; Park, S. H.; Qian, D. J.; Kwon, Y. S. *Curr. Appl Phys.* **2009**, *9*, E232–E234.
(51) Lin, Y. H.; Lu, F.; Tu, Y.; Ren, Z. F. *Nano Lett.* **2004**, *4*, 191–195.
(52) Peng, Y.; Jiang, D. L.; Su, L.; Zhang, L.; Yan, M.; Du, J. J.; Lu, Y. F.; Liu, Y. N.; Zhou, F. M. *Anal. Chem.* **2009**, *81*, 9985–9992.
(53) Razmi, H.; Mohammad-Rezaei, R.; Heidari, H. *Electroanalysis* **2009**, *21*, 2355–2362.
(54) Shi, C. G.; Xu, J. J.; Chen, H. Y. *J. Electroanal. Chem.* **2007**, *610*, 186–192.
(55) Xiao, Y.; Ju, H. X.; Chen, H. Y. *Anal. Chim. Acta* **1999**, *391*, 73–82.
(56) Moattisirat, D.; Velho, G.; Reach, G. *Biosens. Bioelectron.* **1992**, *7*, 345–352.
(57) Wang, H. Y.; Mu, S. L. *Sens. Actuators, B* **1999**, *56*, 22–30.
(58) Bokoch, M. P.; Devadoss, A.; Palencsar, M. S.; Burgess, J. D. *Anal. Chem. Acta* **2004**, *519*, 47–55.
(59) Lyon, J. L.; Stevenson, K. J. *Anal. Chem.* **2006**, *78*, 8518–8525.
(60) Mani, V.; Chikkaveeraiah, B. V.; Patel, V.; Gutkind, J. S.; Rusling, J. F. *ACS Nano* **2009**, *3*, 585–594.
(61) Luo, Y. P.; Liu, H. Q.; Rui, Q.; Tian, Y. *Anal. Chem.* **2009**, *81*, 3035–3041.
(62) Holt, R. E.; Cotton, T. M. *J. Am. Chem. Soc.* **1989**, *111*, 2815–2821.
(63) Yang, M. S.; Chung, F. L.; Thompson, M. *Anal. Chem.* **1993**, *65*, 3713–3716.
(64) Dunford, H. B.; Stillman, J. S. *Coord. Chem. Rev.* **1976**, *19*, 187–251.
(65) Gajhede, M.; Schuller, D. J.; Henriksen, A.; Smith, A. T.; Poulos, T. L. *Nat. Struct. Biol.* **1997**, *4*, 1032–1038.
(66) Dai, Z.; Bao, J.; Yang, X.; Ju, H. *Biosens. Bioelectron.* **2008**, *23*, 1070–1076.
(67) Matsuo, T.; Hayashi, A.; Abe, M.; Matsuda, T.; Hisaeda, Y.; Hayashi, T. *J. Am. Chem. Soc.* **2009**, *131*, 15124–15125.
(68) Zhu, A. W.; Tian, Y.; Liu, H. Q.; Luo, Y. P. *Biomaterials* **2009**, *30*, 3183–3188.
(69) Apel, P. Y.; Korchev, Y. E.; Siwy, Z.; Spohr, R.; Yoshida, M. *Nucl. Instrum. Methods Phys. Res., Sect. B* **2001**, *184*, 337–346.
(70) Ali, M.; Bayer, V.; Schiedt, B.; Neumann, R.; Ensinger, W. *Nanotechnology* **2008**, *19*, 485711.
(71) Wolf-Reber, A. PhD Dissertation, Johann Wolfgang Goethe-Universität Frankfurt am Main, Germany, 2002; ISBN, 3-89825-89490-89829, dissertation.de.
(72) Hermanson, G. T. *Bioconjugate Techniques*; Academic Press: San Diego, 1996.
(73) Cervera, J.; Schiedt, B.; Neumann, R.; Mafe, S.; Ramirez, P. *J. Chem. Phys.* **2006**, *124*, 104706.
(74) Cervera, J.; Schiedt, B.; Ramirez, P. *Europhys. Lett.* **2005**, *71*, 35–41.
(75) Siwy, Z.; Fulinski, A. *Phys. Rev. Lett.* **2002**, *89*, 198103.
(76) Ali, M.; Mafe, S.; Ramirez, P.; Neumann, R.; Ensinger, W. *Langmuir* **2009**, *25*, 11993–11997.
(77) Ali, M.; Ramirez, P.; Mafe, S.; Neumann, R.; Ensinger, W. *ACS Nano* **2009**, *3*, 603–608.
(78) Ali, M.; Yameen, B.; Cervera, J.; Ramirez, P.; Neumann, R.; Ensinger, W.; Knoll, W.; Azzaroni, O. *J. Am. Chem. Soc.* **2010**, *132*, 8338–8348.
(79) Siwy, Z.; Gu, Y.; Spohr, H. A.; Baur, D.; Wolf-Reber, A.; Spohr, R.; Apel, P.; Korchev, Y. E. *Europhys. Lett.* **2002**, *60*, 349–355.
(80) Vlassiouk, I.; Siwy, Z. S. *Nano Lett.* **2007**, *7*, 552–556.
(81) Ali, M.; Schiedt, B.; Healy, K.; Neumann, R.; Ensinger, W. *Nanotechnology* **2008**, *19*, 085713.
(82) Siwy, Z.; Apel, P.; Dobrev, D.; Neumann, R.; Spohr, R.; Trautmann, C.; Voss, K. *Nucl. Instrum. Methods Phys. Res., Sect. B* **2003**, *208*, 143–148.
(83) Siwy, Z. S. *Adv. Funct. Mater.* **2006**, *16*, 735–746.
(84) Radi, A. E.; Munoz-Berbel, X.; Cortina-Puig, M.; Marty, J. L. *Electroanalysis* **2009**, *21*, 1624–1629.
(85) Shannon, L. M.; Kay, E.; Lew, J. Y. *J. Biol. Chem.* **1966**, *241*, 2166–2172.
(86) Su, X.; Teh, H. F.; Lieu, X. H.; Gao, Z. Q. *Anal. Chem.* **2007**, *79*, 7192–7197.
(87) Kadnikova, E. N.; Kostic, N. M. *J. Mol. Catal. B: Enzym.* **2002**, *18*, 39–48.
(88) Rodriguez-Lopez, J. N.; Lowe, D. J.; Hernandez-Ruiz, J.; Hiner, A. N. P.; Garcia-Canovas, F.; Thorneley, R. N. F. *J. Am. Chem. Soc.* **2001**, *123*, 11838–11847.
(89) Korchev, Y. E.; Bashford, C. L.; Alder, G. M.; Apel, P. Y.; Edmonds, D. T.; Lev, A. A.; Nandi, K.; Zima, A. V.; Pasternak, C. A. *FASEB J.* **1997**, *11*, 600–608.
(90) Wolf, A.; Siwy, Z.; Korchev, Y. E.; Reber, N.; Spohr, R. *Cell. Mol. Biol. Lett.* **1999**, *4*, 553–565.
(91) Cadarso, V. J.; Fernandez-Sanchez, C.; Llobera, A.; Darder, M.; Dominguez, C. *Anal. Chem.* **2008**, *80*, 3498–3501.
(92) Powell, M. R.; Sullivan, M.; Vlassiouk, I.; Constantin, D.; Sudre, O.; Martens, C. C.; Eisenberg, R. S.; Siwy, Z. S. *Nat. Nanotechnol.* **2008**, *3*, 51–57.
(93) Ali, M.; Nguyen, Q. H.; Neumann, R.; Ensinger, W. *Chem. Commun.* **2010**, *46*, 6690–6692.
(94) "Protein Data Bank": Berglund, G. I.; Carlsson, G. H.; Smith, A. T; Szoke, H.; Henriksen, A.; Hajdu, J. *Nature* **2002**, *417*, 463–468.